Aquatic Toxicology 241 (2021) 106015

Contents lists available at ScienceDirect

Aquatic Toxicology

journal homepage: www.elsevier.com/locate/aqtox

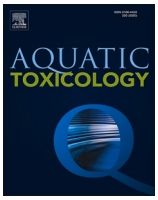

Development of a toxicokinetic-toxicodynamic model simulating chronic copper toxicity to the Zebra mussel based on subcellular fractionation

T.T. Yen Le [a,*], Daniel Grabner [a], Milen Nachev [a], Míriam R. García [b], Eva Balsa-Canto [b], Willie J. G.M. Peijnenburg [c,d], A.Jan Hendriks [e], Bernd Sures [a]

[a] Department of Aquatic Ecology and Centre for Water and Environmental Research (ZWU), Faculty of Biology, University of Duisburg-Essen, D-45141 Essen, Germany
[b] Process Engineering Group, Spanish Council for Scientific Research, IIM-CSIC, 36208 Vigo, Spain
[c] Center for Safety of Substances and Products, National Institute for Public Health and the Environment, Bilthoven, 3720 BA, the Netherlands
[d] Institute for Environmental Sciences, Leiden university, 2311 EZ Leiden, the Netherlands
[e] Department of Environmental Science, Faculty of Science, Radboud University Nijmegen, 6525 HP Nijmegen, the Netherlands

ARTICLE INFO

Keywords:
Subcellular partitioning
Oxidative stress
Chronic toxicity
Biomarkers
Toxicokinetic-toxicodynamic model
Detoxification

ABSTRACT

A toxicokinetic-toxicodynamic model based on subcellular metal partitioning is presented for simulating chronic toxicity of copper (Cu) from the estimated concentration in the fraction of potentially toxic metal (PTM). As such, the model allows for considering the significance of different pathways of metal sequestration in predicting metal toxicity. In the metabolically available pool (MAP), excess metals above the metabolic requirements and the detoxification and elimination capacity form the PTM fraction. The reversibly and irreversibly detoxified fractions were distinguished in the biologically detoxified compartment, while responses of organisms were related to Cu accumulation in the PTM fraction. The model was calibrated using the data on Cu concentrations in subcellular fractions and physiological responses measured by the glutathione S-transferase activity and the lipid peroxidation level during 24-day exposure of the Zebra mussel to Cu at concentrations of 25 and 50 μg/L and varying Na^+ concentrations up to 4.0 mmol/L. The model was capable of explaining dynamics in the subcellular Cu partitioning, e.g. the trade-off between elimination and detoxification as well as the dependence of net accumulation, elimination, detoxification, and metabolism on the exposure level. Increases in the net accumulation rate in the MAP contributed to increased concentrations of Cu in this fraction. Moreover, these results are indicative of ineffective detoxification at high exposure levels and spill-over effects of detoxification.

1. Introduction

Metal bioaccumulation can be estimated fairly well by biokinetic modelling approaches. It is likely, however, that the total body burden of metals in organisms is not indicative of adverse effects or of tolerance to metal exposure (Rainbow, 2002, 2007; Vijver et al., 2004; de Paiva Magalhaes et al., 2015). This is attributed to the chelation of accumulated metals by various subcellular ligands. In association with insoluble metal-rich granules (MRG) or heat-stable proteins in the cytosol (metallothionein-like proteins MTLP), metals are detoxified and cannot modulate metabolism (Wallace et al., 2003; Vijver et al., 2004; Rainbow and Luoma, 2011a). Adverse effects are induced only when metals interact with physiologically sensitive molecules (e.g. small peptides, heat-denatured proteins or enzymes, DNA and RNA) or organelles (mitochondria, nuclei, and membranes) (Mason and Jenkins, 1995; Wallace et al., 2003; Vijver et al., 2004; Wang and Rainbow, 2006; Wang and Wang, 2008a,b; Campbell and Hare, 2009). Therefore, subcellular partitioning is an essential factor determining the impacts of metal bioaccumulation.

With fractionation techniques, the biologically detoxified fraction is usually distinguished from the metabolically available pool (MAP). Metal partitioning to subcellular fractions is a dynamic process (Campana et al., 2015), requiring modelling approaches for a mechanistic understanding. Quantifying the relationship between toxicity and the exceedance of a threshold level of metal accumulation in specific identifiable subcellular fractions is still a challenge in modelling metal biodynamics. While the amount of detoxified metal has been quantified (Wallace et al., 2003; Rainbow and Luoma, 2011a; Rainbow and Smith, 2013), the amount of potentially toxic metal is still not empirically assessed.

* Corresponding author at: University of Duisburg-Essen: Universitat Duisburg-Essen, Essen, Germany.
E-mail address: yen.le@uni-due.de (T.T.Y. Le).

https://doi.org/10.1016/j.aquatox.2021.106015
Received 19 June 2021; Received in revised form 4 October 2021; Accepted 29 October 2021
Available online 2 November 2021

With the potential to simulate the time-course processes that determine adverse effects on organisms, toxicokinetic-toxicodynamic (TK-TD) models have been developed for predicting biological responses (Veltman et al., 2014; Tan et al., 2019). In previously developed TK-TD models, lethal endpoints, such as survival, are mostly related to changes in the body concentration (Ausher et al., 2013; Gao et al., 2015; Tan et al., 2019). This predictor parameter might, however, not appropriately represent the effective internal concentration, attributed to detoxification mechanisms within organisms as mentioned above. An integration of subcellular metal partitioning into TK-TD models might provide a better estimate of metal concentrations at sites of toxic action, and subsequently, more reliable chronic toxicity predictions, as demonstrated by Tan and Wang. (2012). However, uncertainties are inherent in applying the model to essential metals like copper (Cu) since the metal fraction in the MAP that is used in metabolic processes is not considered.

Copper accumulation and consequent toxicity to freshwater mussels, such as the Zebra mussel *Dreissena polymorpha*, are of great interest in ecotoxicology as explained in Le et al. (2021a). Lipid peroxidation is a major mode of toxic action by oxygen radicals generated from Cu-catalysed Fenton/Haber reactions (Nishikawa et al., 1997; Rikans and Hornbrook, 1997; Vijayavel et al., 2007). In response to oxidative stress, organisms stimulate glutathione metabolism and other antioxidant enzymes (de Paiva Magalhaes et al., 2015). For instance, glutathione S-transferase (GST) can prevent oxidative stress by reducing reactive oxygen species (ROS) to alcohol in combination with the oxidation of glutathione (Hayes et al., 2005; Regoli and Giuliani, 2014). The present study aimed to develop a TK-TD model based on subcellular partitioning, considering both detoxification and metabolism, for predicting the GST activity and the LPO level in the Zebra mussel in response to chronic exposure to dissolved Cu. Given the potential influence of Na^+ on Cu toxicokinetics as well as the unique sensitivity of the Zebra mussel to the external ionic composition as elaborated in Le et al. (2021a), the model was calibrated with the data generated from the exposure experiments at different Na^+ concentrations in water or varying salinity levels.

2. Materials and methods

2.1. Model development

2.1.1. Model characterisation

In the model developed in the present study, biological responses were assumed to be related to the accumulation of excess metal (i.e. above the metabolic requirement in combination with the detoxification and elimination capacity) in the MAP, which occurs as a balance of uptake, metabolism, elimination, and detoxification. The assumption is based on the results from previous studies, showing that sublethal effects of Cu were related to the build-up of Cu in non-detoxified pools (Rainbow and Smith, 2013). For essential metals, metabolically available species could be used for metabolic processes. Therefore, in the model developed herein, this fraction was distinguished from the potentially toxic pool. In other words, the metal fraction in excess of metabolic requirements, detoxification, and elimination was defined as potentially toxic metal (PTM; Fig. S1).

Toxicokinetic phase. Metals were assumed to be first accumulated in the MAP (Rainbow, 2002; Wang and Rainbow, 2006) with a rate constant k_{map} (L/g/d) (Fig. S1). This assumption is based on the previous findings that metals are transferred from the sensitive fraction to the inactive or detoxified fraction (Ng and Wang, 2005). Accordingly, accumulated metals are divided into two fractions (Vijver et al., 2004; Luoma and Rainbow, 2008; Rainbow and Luoma, 2011b). In the present model, the detoxified and metabolically available pools are distinguished. The term "metabolically available pool" was used instead of "metal-sensitive fraction" to avoid the confusion that all metals in this fraction are potentially toxic. In the MAP, metals are divided into the metabolic fraction (C_{ME}), i.e. metals are required for essential metabolic processes at a rate constant k_{me} (1/d), and the PTM fraction (C_{PTM}). Metals in the PTM fraction can be reversibly detoxified by binding to MTLP at a rate constant k_{rD} (1/d) (forming the reversibly detoxified or MTLP fraction; C_{MTLP}), irreversibly detoxified via association with MRG with a rate constant k_{iD} (1/d) (forming the irreversibly detoxified or MRG fraction C_{MRG}), which together compose the fraction of biologically detoxified metal (BDM), or eliminated with a rate constant $k_{e,ptm}$ (1/d). Reversibly detoxified metals can be released back to the MAP (k_r; 1/d) in which they can be used in metabolism. Irreversibly detoxified metals in the MRG fraction can be excreted following the elimination of the granules ($k_{e,mrg}$; 1/d) (Vijver et al., 2004). Moreover, reversibly detoxified metals in binding to cysteine-rich proteins like metallothioneins can be broken down in a lysosome, ending up concentrated in MRG (represented by the rate constant k_{int}; 1/d) (Luoma and Rainbow, 2008). The above simulation was based on the previous observation that essential metals can be excreted from the excess fraction or from the detoxified fraction (Rainbow, 2002). Considering the above processes, metal accumulation in the PTM pool occurs as a function of uptake, metabolism, detoxification, and elimination in the following form:

$$\frac{dC_{PTM}}{dt} = k_{map} \times C_w + k_r \times C_{MTLP} - \frac{dC_{ME}}{dt} - \left(k_{rD} + k_{iD} + k_{e,ptm}\right) \times C_{PTM} \quad (1)$$

where C_{PTM}, C_{ME}, and C_{MTLP} (μg/g dw) are metal concentrations in the PTM, metabolic, and reversibly detoxified (via binding to MTLP) fractions, respectively; k_{map} (L/g/d) is the net accumulation rate constant in the MAP; C_W (μg/L) is the dissolved Cu concentration; k_r (1/d) is the rate constant for the release of reversibly detoxified metals from binding to MTLP; k_{rD} (1/d) and k_{iD} (1/d) are the rate constants for reversible and irreversible detoxification, respectively; and $k_{e,ptm}$ (1/d) is the rate constant for metal elimination from the PTM fraction. The metabolic fraction was simulated considering the metabolic requirements by organisms as the maximum concentration in this fraction, as applied for modelling Na^+ influx by Veltman et al. (2014) or for modelling Na^+ binding to Na^+/K^+-ATPase enzymes by Le et al. (2021b) :

$$\frac{dC_{ME}}{dt} = k_{me} \times C_{PTM} \times \left(1 - \frac{C_{ME}}{Me_{max}}\right) \quad (2)$$

with C_{ME} (μg/g dw) being the concentration of metals used in metabolism, which is a function of the metabolism rate (k_{me}; 1/d) and the concentration of metals in the PTM fraction (C_{PTM}) while being restricted by the maximum metabolic requirements Me_{max} (μg/g dw).

Integrating Eq. (2) to Eq. (1) yields:

$$\frac{dC_{PTM}}{dt} = k_{map} \times C_w + k_r \times C_{rD} - k_{me} \times C_{PTM} \times \left(1 - \frac{C_{ME}}{Me_{max}}\right) - \left(k_{rD} + k_{iD} + k_{e,ptm}\right) \times C_{PTM} \quad (3)$$

The maximum metabolic requirements represent the maximum concentration of Cu used in metabolic processes. Measurements of Cu concentrations in the MAP of the mussels living in a Cu-depleted

environment cannot appropriately reflect this parameter. Instead, the parameterisation for this factor is based on theoretical estimates of metabolic requirements by White and Rainbow (1985). Metabolic requirements for essential metals have been elaborated to include requirements for enzymes and for respiratory pigment proteins (White and Rainbow, 1985). Within the bivalvia, hemocyanins are restricted to the Protobranchia (Markl, 2013) while the ancestors of the other bivalves lost their hemocyanins during evolution to adapt to their sessile filter-feeding life style (Markl, private communication). Therefore, an estimate of 26.3 μg/g dw for the enzyme requirements was deployed to represent the maximum metabolic requirements for Cu in the Zebra mussel (excluding haemocyanins).

Metal accumulation in the metabolic and PTM fractions forms the MAP:

$$C_{MAP} = C_{ME} + C_{MTP} \quad (4)$$

Metal concentrations in the reversibly (C_{MTLP}; μg/g dw) and irreversibly (C_{MRG}; μg/g dw) detoxified fractions could be expressed by similar mass-balance equations:

$$\frac{dC_{MTLP}}{dt} = k_{rD} \times C_{PTM} - k_{int} \times C_{MTLP} - k_r \times C_{MTLP} \quad (5)$$

$$\frac{dC_{MRG}}{dt} = k_{iD} \times C_{PTM} + k_{int} \times C_{MTLP} - k_{e,iD} \times C_{MRG} \quad (6)$$

with k_{rD} (1/d) and k_{iD} (1/d) being detoxification rate constants; k_{int} (1/d) representing the incorporation of reversibly detoxified metal to MRG; and $k_{e,iD}$ (1/d) being the rate constant for metal elimination from the irreversibly detoxified fraction.

As such, in the MAP, the metabolic fraction was distinguished from the excess fraction that is potentially toxic. This method is based on previous suggestions that part of the internal metal pool is required for metabolism whereas the pool exceeding the metabolic requirements is potentially toxic (Rainbow, 2002). Considering the toxicological irrelevance of metal accumulation in the cellular debris (Cain et al., 2004; Buchwalter et al., 2008), the cellular debris was not included in the model (Fig. S1).

Toxicodynamic phase. In previous models, lethal endpoints were simulated based on the change in the internal concentration according to a differential equation considering a lower threshold level of acute toxicity (Tan and Wang, 2012; Ashauer et al., 2013; Tan et al., 2019). However, changes in biomarkers were observed even at background concentrations in the environment (see the Discussion section). Therefore, a lower threshold level was not included. Accordingly, the GST activity and the LPO level were related to the Cu concentration in the PTM fraction by the following equations, considering the potential recovery of antioxidant defence systems:

$$\frac{dGST}{dt} = k_{acGST} \times C_{PTM} - k_{reGST} \times GST \quad (7)$$

$$\frac{dLPO}{dt} = k_{acLPO} \times C_{PTM} - k_{reLPO} \times LPO \quad (8)$$

where k_{acGST} and k_{acLPO} (units of GST or LPO/(μmol/g dw)/d) are the rate constants for damage accrual; and k_{reGST} and k_{reLPO} (1/d) regard the

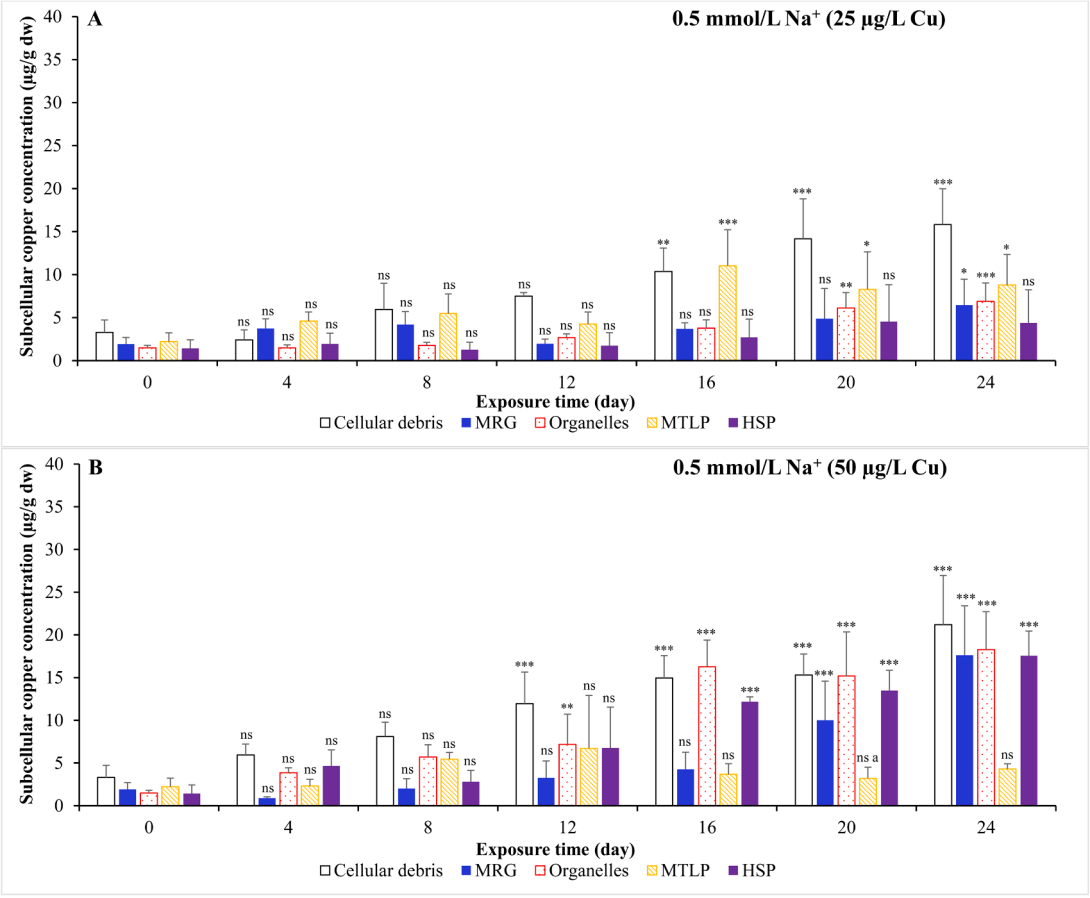

Fig. 1. Copper concentrations (average ± standard deviation) in subcellular fractions: Cellular debris; Metal-rich granules (MRG); Organelles; Metallothionein-like proteins (MTLP); and Heat-sensitive proteins (HSP) in zebra mussels exposed to Cu at 25 and 50 μg/L and Na^+x002B at 0.5 mmol/L. Signs representing significant increases in Cu concentrations in exposed mussels compared to unexposed mussels: ns: non-significant, * ($p < 0.05$), ** ($p < 0.01$), and *** ($p < 0.001$). The results at the other Na^+x002B concentrations are given in Fig. S3.

damage recovery rate constants.

2.1.2. Model calibration

Model calibration was implemented using the MATLAB-based AMIGO2 toolbox as applied previously (Le et al., 2021b). The model was calibrated with data on: 1) the dissolved Cu concentration in water (Table S1, Supporting Information); 2) the Cu concentration in subcellular fractions (Fig. 1 and Fig. S3, Supporting Information); and 3) the GST activity and the LPO level (Tables S2 and S3, Supporting Information). Considering the potential effects of the Na^+ concentration in water or the salinity level on Cu toxicokinetics and responses of the Zebra mussel (see Le et al., 2021a), the model calibration was conducted with data generated from exposure experiments with different Na^+ concentrations in water as described in the following section. Based on results from previous studies (e.g. Tan et al., 2019), the elimination rate was assumed to be independent of salinity. In addition, our previous models (Le et al., 2021a,b) revealed the dependence of elimination on the exposure level. Therefore, in the model calibration, the elimination rate was assumed to be influenced by the Cu exposure level, but not the Na^+ concentration in water. Because of limited interactions between Cu and Na^+ in the intracellular trafficking and transport compared to major interactions in the initial adsorption onto the epithelial cells and the apical/mucosal membranes (Handy et al., 2002), the processes that determine subcellular partitioning (i.e. detoxification, elimination, and metabolism) were assumed not to be influenced by salinity at the narrow range of salinity level investigated. By contrast, the influence of the Cu exposure level on these processes was included in the model. At a narrow range, the GST activity and the LPO level in the zebra mussels were found not to be influenced by Na^+ up to 4.0 mmol/L in water (corresponding to a salinity level up to 0.25 ppt) as shown by an overlap of their ranges (average ± standard deviation) displayed in Tables S2 and S3, Supporting Information. Therefore, parameters in the TD phase were assumed to be independent of salinity in such a narrow range.

2.2. Generation of data for model calibration

2.2.1. Exposure experiments

Zebra mussels were exposed to dissolved Cu at varying conditions in terms of the Cu exposure level and the Na^+ concentration in water. In brief, four sets of treatments were prepared corresponding to four concentrations of Na^+ added to reconstituted water (0.5, 1.5, 2.7, and 4.0 mmol/L). Each set included one control and two treatments in which Cu was added to the organic matter-free reconstituted water at nominal concentrations of 25 and 50 μg/L. After two-week acclimation in a maintenance tank filled with reconstituted water, a group of 40 individuals was randomly sampled for measurements of initial conditions. Simultaneously, the remaining mussels were randomly distributed to the control and exposure tanks. During the 24-day exposure, water was renewed daily. Water samples were taken before and after water renewal for determining dissolved Cu concentrations in the tanks (Le et al., 2021a). Once in four days, mussels were sampled for measurements of GST activity and LPO as well as for analysing subcellular Cu fractionation. No mortality was observed during the exposure for those treatments. Moreover, the stability of the condition index over time and no significant difference in this criterion between control and Cu-exposed mussels (see Le et al., 2021a) indicate a negligible influence of the exposure conditions on the nutrition status of the mussel.

2.2.2. Subcellular fractionation and metal analysis

The subcellular fractionation was implemented following the approach developed by Wallace et al. (2003). In brief, mussel soft tissue was homogenised in cold 20 mM TRIS buffer (pH 7.6), and subsequently centrifuged at 1,450 × *g* and 4°C for 15 min. The supernatant was transferred to a new centrifuge tube for further processing. The resulting pellet was digested in 1 M NaOH at 90 to 95°C for 10 min in a water bath. The mixture was then centrifuged at 5,000 × *g* and 20°C for 10 min to separate MRG as pellets and cellular debris in the supernatant. The supernatant from the 1,450 × *g* centrifugation was centrifuged at 100, 000 × *g* and 4°C for one hour to separate the organelle fraction in the pellet from the cytosol in the supernatant. The supernatant was heated at 80°C in a water bath for 10 min and subsequently centrifuged at 30, 000 × *g* and 4°C for 30 min after cooling for one hour in ice to separate heat-sensitive proteins (HSP, mainly enzymes) in the pellet and heat-stable proteins (or MTLP) in the supernatant. Procedural blanks, i.e. without mussel tissues, were processed using the same protocol to consider the correction due to laboratory and equipment contamination.

Each fraction was dried and added jointly with 4 mL HNO_3 (65%, sub-boiled) in 30 mL Teflon vessels (MarsXpress; CEM GmbH, Kamp-Lintfort, Germany). The vessels were heated up to 170°C for 30 min using a MARS 6 microwave digestion system (CEM GmbH, Kamp-Lintfort, Germany). Concentrations of Cu in the digested samples as well as in water samples were analysed using a Perkin-Elmer-Sciex DRC-e inductively coupled plasma mass spectrometer as described in our previous studies (Le et al., 2021a). Copper was recovered from certified reference materials, i.e. oyster tissue (Standard Reference Material 1566b, Department of Commerce, USA), IAEA-407 (Fish Homogenate Reference Material, International Atomic Energy, Monaco), and DORM-2 (Dogfish Muscle Certified Reference Material, National Research Council, Canada), at the rates of 97–105%.

2.2.3. Measurements of biomarkers

Soft tissues removed from the frozen mussels were homogenised in TRIS buffer containing 10 mM sodium phosphate buffer saline at pH 7.4 at a ratio of 1:10 w/v using an UltraTurrax tissue homogeniser. The homogenates were centrifuged at 14,000 × *g* and 4°C for 15 min. Three aliquots of the supernatant were used for measurements of the biomarkers. Eight replicates (eight individuals) were processed for the sample taken from the maintenance tank prior to the exposure experiment as well as the samples taken from the control and exposure tanks during the exposure. The total protein concentration was spectrophotometrically quantified according to Lowry et al. (1951) with Bovine Serum Albumin as a standard using the Tecan Infinite® 200 PRO microplate reader.

Glutathione-S-transferase activity. The GST activity was determined according to Habig et al. (1974) by spectrophotometrically measuring the increase in absorbance of the acceptor substrate 1-chloro-2,4-dinitrobenzene (CDNB, Sigma Aldrich) with reduced glutathione over time using the Infinite microplate reader (Tecan Infinite® 200 PRO). A reagent mix was freshly prepared from the phosphate buffer (pH 6.5), 200 mM CDNB, and 200 mM glutathione with the ratio of 980:10:10 v/v/v. An aliquot of 5 μL of the sample was mixed with the reagent mixture to obtain a final volume of 200 μL. GST activity was determined from the absorbance measured at 340 nm every 30 s over a period of 4.5 min using a molar extinction coefficient of 9.6 mM^{-1} cm^{-1}.

Lipid peroxidation. Lipid peroxidation was evaluated based on the formation of 2-thiobarbituric acid reactive substances (TBARS) (Buege and Aust, 1978). These peroxide products were determined by reference to the absorbance of malonedialdehyde (MDA) standards (Ohkawa et al., 1979). A mixture was obtained by mixing tissue homogenate (110 μL) with 27.5 μL of 8.1% sodium dodecyl sulfate and subsequently with 440 μL of the staining agent (containing 10% trichloric acid pH 3.5 and 0.5% thiobarbituric acid), and boiled in a water bath at 95°C for 20 min. After cooling, the vigorously-shaken mixture was centrifuged at 4,000 × *g* and 4°C for 10 min. The absorbance of the obtained supernatant was spectrophotometrically measured at 532 nm using the Tecan Infinite® 200 PRO microplate reader. The concentration of TBARS was determined from an external standard curve of 1,1,3,3-tetramethoxy propane (a stabilised form of MDA).

3. Results

3.1. Dynamics in the subcellular partitioning of copper in the Zebra mussel

In non-exposed mussels, Cu concentrations in the subcellular fractions stabilised during the experiment (Fig. S2). In general, at a nominal exposure concentration of 25 μg/L, the Cu concentration in subcellular fractions gradually increased during the 24-day exposure (Fig. 1A and Fig. S3C-E-G). In these treatments, contrasting with an evident trend of the increased concentration in the cellular debris and the organelles, higher fluctuations were seen in the changes of the Cu concentration in the other subcellular fractions (Fig. 1A and Fig. S3C-E-G). A similar pattern was recorded in the exposure to Cu at 50 μg/L (Fig. 1B and Fig. S3D-F-H). Generally, Cu was accumulated in the subcellular fractions in concentrations that increased as follows: cellular debris > organelles > MTLP > MRG > HSP (Fig. 1 and Fig. S3).

The Bartlett's test and the D'Agostino & Pearson omnibus test demonstrated that the data fulfilled the assumptions of homogeneity of variance and normal distribution. In order to remedy the issue of pseudoreplication when individuals of mussels were sampled from the same treatment tank, average values for all the individuals were used in the analysis of variance (ANOVA) test as suggested by Lazic (2010). According to the two-way (exposure time and treatment) analysis of variance (ANOVA) followed by the Bonferroni post-test with GraphPad Prism, exposure to Cu significantly affected Cu concentrations in all subcellular fractions ($p < 0.0001$). Such influence depended on exposure time and varied amongst fractions (Fig. 1 and Fig. S3). Exposure time and treatment had significant interactive effects on Cu accumulation in the cellular debris, organelle, and MRG fractions ($p < 0.0001$; Fig. 1 and Fig. S3). Significant increases in Cu concentrations in these fractions were more frequently noticed at the last exposure period (Fig. 1 and Fig. S3). Exposure time had a non-significant influence on the concentration of Cu bound to MTLP (Fig. 1 and Fig. S3). On the contrary, treatments with varying Cu exposure levels had significant impacts on the Cu concentration in the MTLP fraction ($p < 0.0001$; two-way ANOVA). Significant increases in the Cu concentration in this fraction of exposed mussels compared to the non-exposed conspecifics were only revealed during the last period (post 12 days; Fig. 1 and Fig. S3). Noticeably, significant increases in the concentration of Cu binding to HSP were only found following exposure at the higher level (Fig. 1 and Fig. S3). According to the two-way (Na^+ concentration in water and exposure time) ANOVA test, at both Cu exposure levels, significant differences in subcellular Cu concentrations between Na^+ levels were only seen at some data points (not shown in Fig. 1 because of a large number of paired comparisons). This was also indicated by overlapping ranges (average ± standard deviation) of Cu concentrations in the subcellular fractions at varying Na^+ concentrations in water (Fig. 1 and Fig. S3).

From the perspective of ecotoxicology, internalised metals were grouped to the cellular debris, MAP, and BDM fractions (Fig. S4). The subcellular partitioning of Cu expressed by its proportions (%) in these fractions depended on the Cu exposure level (Fig. S4). In particular, increases in the proportion of the MAP with increasing exposure levels from 25 to 50 μg/L (two-way ANOVA test: $p<0.05$) were accompanied by decreases in the distribution to the BDM fraction (two-way ANOVA test: $p<0.05$), except for in the solution added with Na^+at 1.5 mmol/L. These patterns led to changes in Cu distribution: at 25 μg/L, detoxified Cu accounted for a higher proportion than sensitive Cu ($p < 0.05$), contrasting with the pattern at 50 μg/L ($p < 0.05$; Fig. S4). On average, the MAP accounted for 28.4% (± 7.8) compared to 36.9% (± 9.7) for the BDM fraction at an exposure of 25 μg/L. At 50 μg/L, 39.4% (± 6.6) of the Cu body burden was distributed to the MAP in comparison to 28.8% (± 5.7) in the BDM. On the contrary, the proportion of internal Cu distributed to the cellular debris did not differ between the two exposure levels (Fig. S4). The dynamics in the subcellular partitioning of Cu in zebra mussels with no clear pattern during the 24-day exposure (Fig. S4) was related to the changes in the distribution with changing whole-body concentrations (Fig. S5). Increases in Cu partitioning to the MAP were correlated with slight decreases in the distribution to the cellular debris and more substantial decreases in the distribution to the BDM pool (Fig. S5). Furthermore, these patterns indicate spill-over effects, which occur when metal uptake exceeds the combination of metabolic requirements and detoxification/elimination capacity. Remarkably, the Cu concentration in the MAP and BDM fractions at equal distribution to these compartments (28.87 μg/g dw; Fig. S5) was slightly higher than the maximum metabolic requirements (26.3 μg/g dw). This result is unambiguous evidence of the regulation by the Zebra mussel at low levels of Cu body burden to meet the metabolic requirements, on the one hand, and to limit the concentration of metals in the PTM fraction or in the MAP by various detoxification mechanisms, on the other hand. When the Cu level in the MAP exceeded the maximum metabolic requirements, the inefficient detoxification capacity led to increasing Cu concentration in the MAP (Fig. S5).

3.2. Toxicokinetic-toxicodynamic model based on subcellular partitioning

The above dynamics in subcellular Cu partitioning was related to the dependence of kinetic parameters on the exposure level, as revealed by model calibration (Table 1). For example, Cu was accumulated in the MAP at a higher rate constant at 50 μg/L Cu (0.09–0.16 L/g/d) than at 25 μg/L (0.05–0.07 L/g/d; Table 1). The dose-dependence was also seen for the rate constants for metal elimination from the PTM or irreversibly detoxified fractions and for metal detoxification (Table 1). Elimination was negligible at the lower exposure level but more profound at the accelerated level in interaction with detoxification. Increases in the elimination rate constant were accompanied by decreases in the detoxification rate constants with increasing exposure level (Table 1). At the lower exposure concentration, Cu from the reversibly detoxified fraction was released back to the MAP with a higher rate constant (Table 1) to fulfil metabolic requirements. In addition, the metabolism rate constant increased with increasing exposure concentration (Table 1). Contrasting with such an influence of the Cu exposure level, the results of model calibration showed that the Cu accumulation rate constant in the MAP was not affected by the concentration of Na^+ in water (Table 1).

The increase in the net accumulation rate in the MAP with increasing exposure level (Table 1) contributed to significantly higher concentrations of Cu in the MAP at 50 μg/L than at 25 μg/L (Fig. S4). By contrast, no significant differences were seen in Cu concentrations in the reversibly (MTLP) and irreversibly detoxified (MRG) fractions between the two exposure levels as represented by an overlap of the estimates (Fig. 2 and Fig. S6). Moreover, this result indicates an occurrence of spill-over effects, which led to the build-up of Cu in the MAP as found above.

Compared to Cu toxicokinetics, higher uncertainty was inherent in predicting Cu toxicodynamics (Table 1). Moreover, GST activity was more sensitive than LPO, as shown by a higher accrual damage rate constant for GST activity than for LPO (Table 1). This observation was further demonstrated by the estimates of GST activity and LPO (Fig. 2 and Fig. S6). In particular, at 25 μg/L Cu, the estimated GST activity slightly increased over time. At 50 μg/L, increases at the initial period were followed by a more stable trend. Lower increases were predicted for the LPO level than for the GST activity (Fig. 2 and Fig. S6). Their fluctuations could not be totally captured by the developed TK-TD model.

4. Discussion

Subcellular metal partitioning is a dynamic process, depending on the interactions between uptake, elimination, detoxification, and metabolism. Dynamics in subcellular partitioning are additionally attributed to the dependence of these processes and their interactions on

Table 1
Estimates for calibrated parameters in the TKTD model based on subcellular metal partitioning: the net accumulation rate constant (k_{map}; L/g/d); the rate constant for the release of reversibly detoxified metal from the binding to metallothionein-like proteins back to the metabolically available pool (k_r; 1/d); the rate constants for reversible detoxification (k_{rD}; 1/d) and irreversible detoxification (k_{iD}; 1/d); the rate constant for incorporation of reversibly detoxified metal into the metal-rich granules (k_{int}; 1/d); the rate constant for elimination of metals from the metabolically available pool ($k_{e,ptm}$; 1/d); the rate constant for metal ustilisation in metabolic processes (k_{me}; 1/d); the rate constant for elimination of irreversibly detoxified metal ($k_{e,mrg}$; 1/d); the damage accurate rate constants for the glutathione-S-transferase activity (k_{acGST}; unit of GST/unit of tissue concentration/d) and for lipid peroxidation (k_{acLPO}; unit of LPO/unit of tissue concentration/d); and the recovery rate constant for the glutathione-S-transferase activity (k_{reGST}; 1/d) and for lipid peroxidation (k_{reLPO}; 1/d) .

Parameter	25 µg/L Cu				50 µg/L Cu			
	0.5 mM Na^+	1.5 mM Na^+	2.7 mM Na^+	4.0 mM Na^+	0.5 mM Na^+	1.5 mM Na^+	2.7 mM Na^+	4.0 mM Na^+
k_{map}	0.05 (± 0.05)	0.06 (± 0.05)	0.05 (± 0.04)	0.07 (± 0.07)	0.09 (± 0.09)	0.13 (± 0.14)	0.13 (± 0.14)	0.16 (± 0.17)
k_r	0.11 (± 0.29)				$5.42 \cdot 10^{-4}$			
k_{rD}	1.00 (± 1.18)				0.86 (± 0.92)			
k_{iD}	$2.05 \cdot 10^{-3}$ (± 0.78)				$5.34 \cdot 10^{-4}$ (± 5.30)			
k_{int}	0.07 (± 0.16)				0.13 (± 0.13)			
$k_{e,ptm}$	0.01 (± 0.90)				1.00 (±3.42)			
k_{me}	0.10 (± 0.30)				0.93 (± 1.48)			
$k_{e,mrg}$	0.13 (± 0.26)				0.51 (± 0.56)			
k_{acGST}	52 (± 109)							
k_{reGST}	0.71 (± 1.93)							
k_{acLPO}	5.80 (± 106)							
k_{reLPO}	2.00 (± 37)							

exposure level and conditions. As proven in the present study, these interactions can be simulated by a TK-TD model. Results of model calibration explained experimentally observed dynamics in subcellular Cu partitioning. For instance, the increases in the net accumulation rate in the MAP with increasing exposure level contributed to the increasing Cu concentration in this fraction, on the one hand, and indicate some limits in the Cu sequestration capacity of this organism, on the other hand. Such limitation may explain the empirical observations of higher Cu concentrations in metabolically available fractions than in detoxified pools in bivalve molluscs, as revealed in the present study and previous research (Voets et al., 2009; Ju et al., 2011). Moreover, such a pattern of subcellular partitioning explains the high sensitivity of this organism to Cu as noticed in other studies (March et al., 2007). At a nominal exposure concentration of 25 µg/L, Cu was accumulated in the MAP at a lower rate (0.05–0.07 L/g/d) than the whole body uptake rate (0.09–0.11 L/g/d; Le et al., 2021b) (Table S4). This is indicative of an ability of this bivalve to detoxify accumulated Cu at this exposure level. Zebra mussels are able to regulate uptake and/or excretion of essential metals, e.g. Cu and Zn, to a certain extent (Bervoets et al., 2004) as supported by lower variations in the tissue concentration of essential metals compared to those for non-essential metals (Voets et al., 2009). However, the detoxification ability is inefficient at elevated exposure levels. For example, with the Na^+ concentration in water ranging from 1.5 to 4.0 mmol/L, Cu was accumulated in the MAP at a higher rate (0.13–0.16 L/g/d) than the uptake rate to the whole body of mussels (0.09–0.14 L/g/d) at a concentration of 50 µg/L (Table S4). Such changes in the comparison between the rate of net accumulation in the MAP and the whole body uptake rate indicate spill-over effects on Cu detoxification, leading to increased accumulation of Cu in the MAP. Ineffective detoxification at high exposure levels was further supported by non-significant differences in the estimates of Cu concentrations in the reversibly and irreversibly detoxified fractions at varying exposure levels. Ineffective detoxification of Cu in zebra mussels was also reported by Voets et al. (2009), as shown by the increasing proportion of Cu in organelles with increasing Cu concentration in the whole body. The impacts of exposure levels on Cu accumulation in the MAP unravelled from empirical observations as well as the model calibration agree with the reported results for Cu whole body uptake from our previous biokinetic and TK-TD models (Le et al., 2021a,b).

The influence of salinity has already been considered in the assessment of metal bioavailability, uptake, and toxicity. The influence has often been interpreted by the competition between toxic cations and 'hard' cations for forming organic and inorganic complexes in the environment and for binding sites on the biotic ligands (Di Toro et al., 2001). The former could be well simulated by speciation models, e.g. WHAM (Tipping, 1998) and visual MINTEQ (Gustafsson, 2011). The chemical speciation with the WHAM VII model for the organic matter-free reconstituted water showed a negligible influence of Na^+ at the concentration range of 0.5 to 4.0 mmol/L on the free ion activity of Cu^{2+}, which represents the most active species. According to the principle of the biotic ligand model, the effects of hard ions on metal binding at biotic ligands could be written as a function of their affinity for these ligands and their concentrations (Le et al., 2012). The non-significant influence of the Na^+ concentration in the present study might be related to the narrow range investigated. In the TK-TD models developed by Chen et al. (2017) and Tan et al. (2019), the rate of Cd uptake by the estuarine clam *Potamocorbula laevis* decreased with increasing salinity level from 5 to 30 ppt. Further discussion on the potential effects of salinity on metal uptake is given in Le et al. (2021a). Previous findings indicated a limited influence of Na^+ on subcellular metal partitioning. Jacobson and Turner (1980) found that hard metal ions generally form the weakest complexes nucleic acids and proteins. Handy et al. (2002) indicated limited interactions between Cu and Na^+ in the intracellular trafficking and transport. These results support our assumption of a negligible influence of salinity or Na^+ on subcellular Cu partitioning.

Subcellular metal partitioning is indicative of metal adaptation strategies of organisms in response to metal exposure. The present study shows that TK-TD models allow for a delineation of adaptation strategies. The opposite changes in the detoxification rate and the elimination rate with changing exposure level or changing whole-body concentration unravelled by our model confirm the trade-off between elimination and detoxification reported in previous studies (Ju et al., 2011). At the lower test concentration, Cu was effectively detoxified by various pathways, limiting the requirement for elimination. According to Ju et al. (2011), the capacity of metal detoxification might complement the limited elimination ability. However, at higher exposure levels, the spill-over effect causes an acceleration of elimination. In agreement with the influence of the exposure level on kinetic parameters in our TK-TD model, Ju et al. (2011) estimated metal uptake, elimination, and detoxification in the MAP for various bivalves. These authors demonstrated variations in these parameters depending on species, metal, and exposure level. According to Ju et al. (2011), the rate constants for Zn uptake and elimination from the MAP in bivalves were positively correlated, contrasting with a lack of a clear trend for Cu. Differences between Cu and Zn were also found for the relationship between the elimination and detoxification rate constants, i.e. a negative correlation for Cu and a positive interaction for Zn (Ju et al., 2011). However, these conclusions need further investigation given the limited data in the

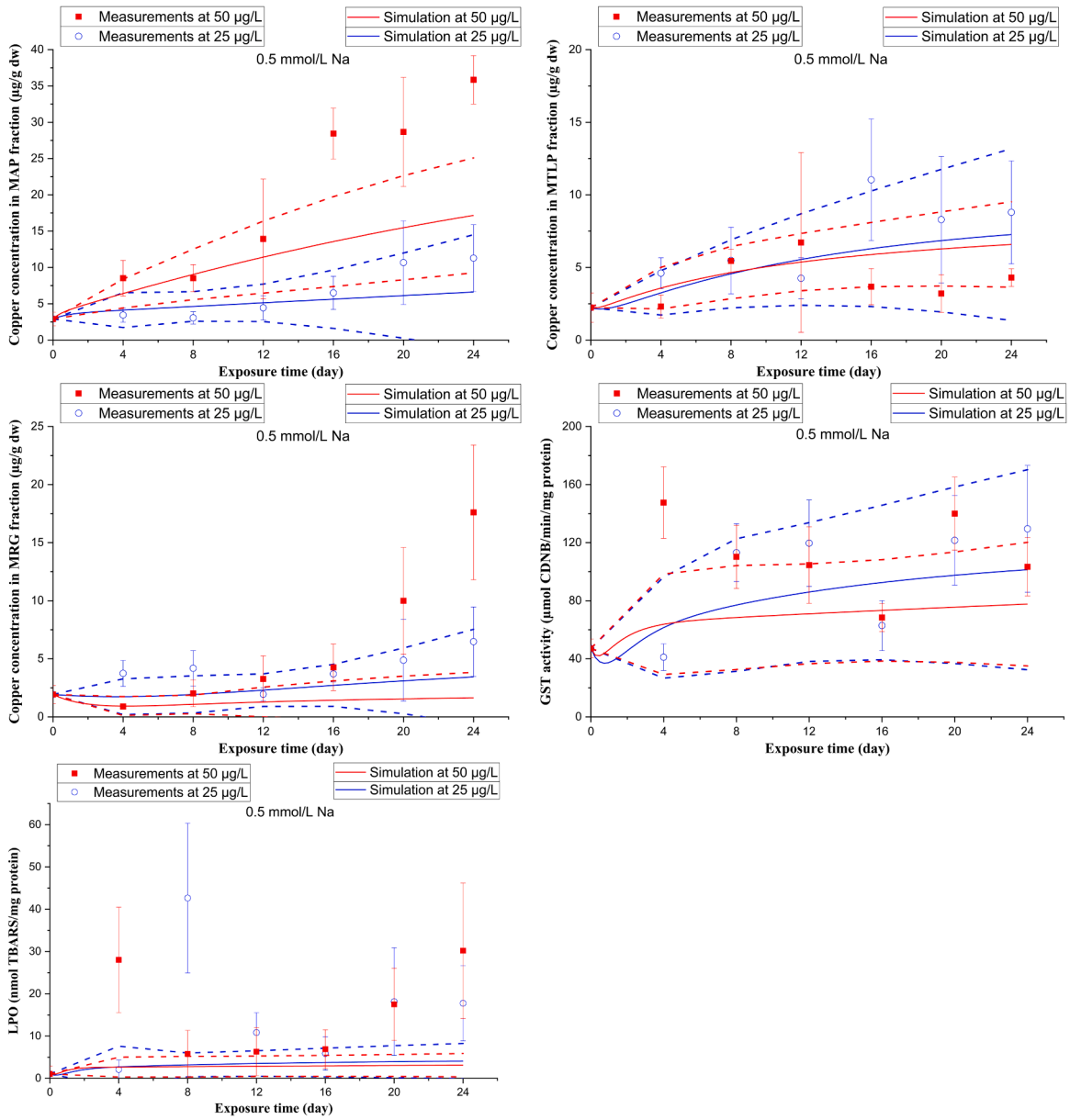

Fig. 2. Relationships between the estimates and the measurements of Cu concentrations in the metabolically available pool (MAP), metallothionein-like protein (MTLP; or reversibly detoxified), and metal-rich granules (MRG; or irreversibly detoxified) fractions, glutathione-S-transferase (GST) activity, and lipid peroxidation (LPO) in the zebra mussel. The dots and bars represent the measurements (average and standard deviations, respectively). The areas covered by the dashed lines represent the confidence interval of the estimate with the solid line in middle representing the mean estimate. The comparison at other Na+ concentrations is give in Fig. S6.

study of Ju et al. (2011). The findings that among the detoxified fractions of the Zebra mussel, Cu was mainly associated with MTLP, which is in agreement with the observation by Voets et al. (2009), could be related to a higher rate of reversible detoxification than the rate of irreversible detoxification (Table 1). Copper was found in sensitive fractions even before the exposure experiment in the present study (Fig. S2). This observation agrees with the findings that there was no threshold level below which excess of Cu was successfully detoxified by the Zebra mussel (Voets et al., 2009) or by the mussel *Pyganodon grandis* (Campbell et al., 2005).

Despite the potential of the developed TK-TD model for capturing the dynamics of subcellular metal partitioning, some limitations were seen in the current version. Compared to the estimation of Cu concentrations in the MAP and in the reversibly detoxified (or MTLP) fraction, substantial deviations were seen between the estimates and the measurements of Cu concentrations in the irreversibly detoxified (MRG) fraction at the last exposure period, corresponding to a high total body burden. On the one hand, the limitation of the model reflects the complexity in the dynamic subcellular partitioning of Cu in bivalves as reported previously. For instance, no correlation was found between Cu concentrations in subcellular fractions or subcellular Cu partitioning with changes in the soft tissue concentration (Voets et al., 2009; Pan and Wang, 2012). For the Zebra mussel, Voets et al. (2009) displayed a lack of a significant relationship between Cu accumulation in MRG and the whole tissue concentration. On the other hand, such limitation might be related to some simulation approaches in the current version of the model. The first potential contributor might be related to the inability of the linear function between the changes in the encapsulation of Cu to the granules and the Cu concentration in the PTM fraction. Previous studies have indicated that at high exposure levels, metal accumulation in the MTLP fraction may be hyperbolic (Brown and Parsons, 1978; Roesijadi, 1980). A similar phenomenon is applicable to metal accumulation in the MRG

fraction, contributing to high deviations between estimated and measured Cu concentrations in this fraction. Another possible contributor to the limitation of the present model version might be related to the characterisation of metal incorporation into inorganic granules with the one-compartment PTM fraction. Previous findings on the time required for metal incorporation into inorganic granules (Brown, 1982; Vijver et al., 2004) are indicative of a time-dependent rate of irreversible detoxification. Accordingly, the simulation of irreversible detoxification with one rate constant as in the model might not describe the kinetic Cu accumulation in the MRG appropriately. Therefore, a hyperbolic function or a two-compartment PTM for slow and quick detoxification via incorporation in MRG might be considered in the future to improve the prediction accuracy.

Uncertainties are inherent in the model, as can be attributed to its assumptions. For example, as a number of assumptions are included in theoretically estimating the metabolic requirements (White and Rainbow, 1985), uncertainties are inherent in deriving the maximum Cu concentration in the metabolic compartment. Besides the needs of co-enzymes, essential metals might be required for other processes. Furthermore, high uncertainty in the TD section indicates challenges in developing TK-TD models for chronic metal toxicity. This uncertainty is attributed to substantial variations in physiological responses to metal exposure at sub-lethal levels. Previous studies did not show a consistent trend in the changes of the GST activity or the LPO level in bivalves in response to metals. For example, Peric et al. (2020) proposed that a lack of alleviative effects on the GST activity and the LPO level might be attributed to the involvement of ROS-scavenging enzymes. Such variations in biomarker responses exert high uncertainty in TD modelling, as exemplified by the relationship between metal concentrations at sites of toxic action and biomarkers in the present study. The uncertainties in the simulation of metal toxicodynamics in chronic sublethal exposure reflect our limited understanding on the relationship between the tissue concentration and biomarker responses in this condition. The use of an ordinary differential equation to represent the relationship between the total tissue concentration or the concentration at target sites and the biological response have usually been applied in TK-TD models estimating acute effects on the time-course survival or mortality of organisms (Jager et al., 2011; Gao et al., 2019; Tan et al., 2019). Further efforts in future studies should be put on obtaining a better understanding of the relationship between metal accumulation in organisms or at target sites and biomarker responses at sublethal levels. Despite the uncertainties in the TD phase, mechanisms of toxicity were explained by the model to some extent. For instance, the higher sensitivity of GST activity (a damage accrual rate constant of 52 units of GST/unit of Cu concentration/d) than LPO (a damage accrual rate constant of 5.8 units of LPO/unit of Cu concentration/d) was consistent with the function of GST to counteract damages, for example inhibiting LPO formation. A lack of a significant increase in the GST activity and LPO in the Zebra mussel in the present study indicates an adequate response of the antioxidant defence system to the generation of ROS. This conclusion was also recently obtained in assessing the response of oysters exposed to Cd (Peric et al., 2020). Furthermore, oxidative stress-related biomarker responses, such as LPO and GST activity, should be related to toxicological effects in the next step. Lipid peroxidation might lead to changes in the physical properties of cellular membranes, covalent modification of proteins and nucleic acids, and consequent cell death and disease (Gaschler and Stockwell, 2017). A link between biomarker responses and such effects in the TD phase facilitates an extrapolation from the subcellular level to higher levels of biological organisation.

Several factors distinguish the model developed in the present study from the previous models that are also based on subcellular partitioning. In previously developed TK-TD models, lethal/acute toxicity was related to metal accumulation in the MAP ignoring the essentiality of metals like Cu to metabolic processes. In the present TK-TD model, responses of organisms were related to metal concentrations in the PTM fraction, considering the metabolic requirements of essential metals. In previous models, a single detoxification rate was used to represent different detoxification mechanisms, whereas differences in properties and the importance of various detoxification mechanisms have been reported (Vijver et al., 2004; Pan and Wang, 2009). A longer time is usually required for the encapsulation of metals in granules (Brown, 1982; Vijver et al., 2004), while the synthesis of metallothioneins can be rapidly induced (Roesijadi, 1992). Accordingly, the induction of metallothioneins is suggested to be of importance in short-term exposure, while the storage in granules plays an essential role in chronic exposure (Vijver et al., 2004). A standard elimination rate was applied in available dynamic models while detoxified metals, such as in granules, tend to be eliminated at a lower rate than organelle- or enzyme-associated metals (Ng and Wang, 2005). In the TK-TD model developed in the present study, the distinction of reversibly and irreversibly detoxified fractions allows for considering differences in characteristics of various detoxification pathways as discussed above. In previous biodynamic models, the onset of toxic effects is assumed to be initiated when the uptake rate exceeds the combined rates of detoxification and elimination (Van Straalen et al., 2005; Rainbow, 2007; Luoma and Rainbow, 2008; Adams et al., 2010; Casado-Martinez et al., 2010; Rainbow and Luoma, 2011a). However, as mentioned above, there is no evidence of the existence of a threshold level below which metals are successfully detoxified. To consider this perspective, the response of the organism was assumed to be determined by metal concentrations in the PTM fraction in the present study. With a general framework based on subcellular metal partitioning, the model can be readily extrapolated to other aquatic organisms and other species.

5. Conclusions

A TK-TD modelling framework based on subcellular metal partitioning was developed for predicting biomarker responses in terms of oxidative stress of the Zebra mussel to chronic exposure to Cu at sublethal levels. The metal concentration in the PTM fraction, which was assumed to represent the metal level at sites of toxic action and directly relate to biological responses, was simulated as a function of uptake, metabolism, detoxification, and elimination. The model allows for: 1) predicting metal accumulation in the PTM fraction; 2) simulating the dynamics of subcellular metal partitioning; and 3) estimating biomarker responses in relation to the changes in metal accumulation in the PTM compartment. The model could explain the time course of metal accumulation in various subcellular fractions as well as the effect mechanism reasonably well. Given the current limitation in our understanding of the tissue concentration-biomarker response relationship in chronic sublethal exposure, simulation approaches should be further explored to reduce uncertainties in the estimation of metal concentrations in subcellular fractions and biomarker responses.

CRediT authorship contribution statement

T.T. Yen Le: Conceptualization, Methodology, Investigation, Validation, Visualization, Writing – original draft, Funding acquisition. **Daniel Grabner:** Methodology, Investigation, Writing – review & editing. **Milen Nachev:** Methodology, Investigation, Writing – review & editing. **Míriam R. García:** Methodology, Writing – review & editing. **Eva Balsa-Canto:** Methodology, Writing – review & editing. **Willie J.G. M. Peijnenburg:** Methodology, Validation, Writing – review & editing. **A.Jan Hendriks:** Validation, Writing – review & editing. **Bernd Sures:** Project administration, Validation, Writing – review & editing.

Declaration of Competing Interest

The authors declare that they have no known competing financial interests or personal relationships that could have appeared to influence the work reported in this paper.

Acknowledgements

This research was financed by the Deutsche Forschungsgemeinschaft (DFG), Germany (LE 3716/2-1). We would like to thank the anonymous reviewers and the Editor for their constructive comments to improve the manuscript.

Supplementary materials

Supplementary material associated with this article can be found, in the online version, at doi:10.1016/j.aquatox.2021.106015.

References

Adams, W.J., Blust, R., Borgmann, U., Brix, K.V., DeForest, D.K., Green, A.S., Meyer, J.S., McGeer, J.C., Paquin, P.R., Rainbow, P.S., Wood, C.M., 2010. Utility of tissue residues for predicting effects of metals on aquatic organisms. Int. Environ. Assess. Manag. 7, 75–98.

Ashauer, R., Thorbek, P., Warinton, J.S., Wheeler, J.R., Maund, S., 2013. A method to predict and understand fish survival under dynamic chemical stress using standard ecotoxicity data. Environ. Toxicol. Chem. 32, 954–965.

Bervoets, L., Voets, J., Chu, S.G., Covaci, A., Schepens, P., Blust, R., 2004. Comparison of accumulation of micropolluatants between indigenous and transplanted zebra mussels (*Dreissena polymorpha*). Enviorn. Toxicol. Chem. 23, 1973–1983.

Brown, B.E., 1982. The form and function of metal-containing "granules" in invertebrate tissues. Biol. Rev. 57, 621–667.

Brown, D.A., Parsons, T.R., 1978. Relationship between cytoplasmic distribution of mercury and toxic effects to zooplankton and chum salmon (*Onchorhynchus keta*) exposed to mercury in a controlled ecosystem. J. Fish. Res. Bd. Can. 35, 880–884.

Buchwalter, D.B., Cain, D.J., Martin, C.A., Xie, L., Luoma, S.N., Garland Jr., T., 2008. Aquatic insect ecophysiological traits reveal phylogenetically based differences in dissolved cadmium susceptibility. Proc. Natl. Acad. Sci. USA 105, 8321–8326.

Buege, J.A., Aust, S.D., 1978. Microsomal lipid peroxidation. Methods Enzymol. 52, 302–310.

Cain, D.J., Luoma, S.N., Wallace, W.G., 2004. Linking metal bioaccumulation of aquatic insects to their distribution patterns in a mining-impacted river. Environ. Toxicol. Chem. 23, 1463–1473.

Campana, O., Taylor, A.M., Maher, W.A., Simpson, S.L., 2015. Importance of subcellular metal partitioning and kinetics to predicting sublethal effects of copper in two deposit-feeding organisms. Environ. Sci. Technol. 49, 1806–1814.

Campbell, P.G.C., Hare, L., 2009. Metal detoxification in freshwater animals. Roles of metallothioneins. In: Sigel, A., Sigel, H., Sigel, R.K.O. (Eds.), Metallothioneins and Related Chelators. Royal Society of Chemistry, Cambridge, UK, pp. 239–277.

Campbell, P.G.C., Giguere, A., Bonneris, E., Hare, L., 2005. Cadmium-handling strategies in two chronically exposed indigenous freshwater organisms – the yellow perch (*Perca flavescens*) and the floater molusc (*Pyganodon grandis*). Aquat. Toxicol. 72, 83–97.

Casado-Martinez, M.C., Smith, B.D., Luoma, S.N., Rainbow, P.S., 2010. Metal toxicity in a sediment-dwelling polychaete: threshold body concentrations or overwhelming accumulation rates? Environ. Pollut. 158, 3071–3076.

Chen, W.-Q., Wang, W.-X., Tan, .Q..-G., 2017. Revealing the complex effects of salinity on copper toxicity in an estuarine clam *Potamocorbula laevis* with a toxicokinetic-toxicodynamic model. Environ. Pollut. 222, 323–330.

de Paiva Magalhaes, D., da Costa, M.R., Baptista, D.F., Buss, D.F., 2015. Metal bioavailability and toxicity in freshwaters. Environ. Chem. Lett. 13, 69–87.

Di Toro, D.M., Allen, H.E., Bergman, H.L., Meyer, J.S., Paquin, P.R., Santore, R.C., 2001. Biotic ligand model of the acute toxicity of metals. 1. Technical basis. Environ. Toxicol. Chem. 20, 2383–2396.

Gao, Y., Feng, J., Zhu, L., 2015. Prediction of acute toxicity of cadmium and lead to zebrafish larvae by using a refined toxicokinetic-toxicodynamic model. Aquat. Toxicol. 169, 37–45.

Gao, Y., Zhang, Y., Feng, J., Zhu, L., 2019. Toxicokinetic-toxicodynamic modeling of cadmium and lead toxicity to larvae and adult zebrafish. Environ. Pollut. 251, 221–229.

Gaschler, M.M., Stockwell, B.R., 2017. Lipid peroxidation in cell death. Biochem. Biophys. Res. Commun. 482, 419–425.

Gustafsson, J.P., 2011. Visual MINTEQ 3.0 User Guide. Royal Institute of Technology, Stockholm, Sweden.

Handy, R.D., Eddy, F.B., Baines, H., 2002. Sodium-dependent copper uptake across epithelia: a review of rationale with experimental evidence from gill and intestine. Biochim. Biophys. Acta. 1566, 104–115.

Hayes, J.D., Flanagan, J.U., Jowsey, I.R., 2005. Glutathione transferases. Annu. Rev. Pharmacol. Toxicol. 45, 51–88.

Habig, W.H., Pabst, M.J., Jakoby, W.B., 1974. Glutathione S-Transferases: the first enzymatic step in mercapturic acid formation. J. Biol. Chem. 249, 7130–7139.

Jacobson, K.B., Turner, J.E., 1980. The interaction of cadmium and certain other metal ions with proteins and nucleic acids. Toxicology 16, 1–37.

Jager, T., Albert, C., Preuss, T.G., Ashauer, R., 2011. General unified threshold model of survival – a toxicokinetic-toxicodynamic framework for ecotoxicology. Environ. Sci. Technol. 45, 2529–2540.

Ju, Y.-R., Chen, W.-Y., Singh, S., Liao, .C..-M., 2011. Trade-offs between elimination and detoxification in rainbow trout and common bivalve molluscs exposed to metal stressors. Chemosphere 85, 1048–1056.

Lazic, S.E., 2010. The problem of pseudoreplication in neuroscientific studies: is it affecting your analysis? Lazic BMC Neurosci. 11, 5.

Le, T.T.Y., Grabner, D., Nachev, M., Peijnenburg, W.J.G.M., Hendriks, A.J., Sures, B., 2021a. Modelling copper toxicokinetics in the zebra mussel, *Dreissena polymrpha*, under chronic exposures at various pH and sodium concentrations. Chemosphere 267, 129278.

Le, T.T.Y., Nachev, M., Grabner, D., Garcia, M.R., Balsa-Canto, E., Hendriks, A.J., Peijnenburg, W.J.G.M., Sures, B., 2021b. Modelling chronic toxicokinetics and toxicodynamics of copper in mussels considering ionoregulatory homeostatis and oxidative stress. Environ. Pollut. 287, 117645.

Le, T.T.Y., Peijnenburg, W.J.G.M., Hendriks, A.J., Vijver, M.G., 2012. Predicting effects of cations on copper toxicity to lettuce (*Lactuca sativa*) by the Biotic Ligand Model. Environ. Toxicol. Chem. 31, 355–359.

Lowry, O.H., Rosebrough, N.J., Farr, A.L., Randall, R.J., 1951. Protein measurement with the folin phenol reagent. J. Biol. Chem. 193, 265–275.

Luoma, S.N., Rainbow, P.S., 2008. Metal Contamination in Aquatic Environments. Science and Lateral Management. Cambridge University Press, Cambridge, UK.

March, F.A., Dwyer, F.J., Augspurger, T., Ingersoll, C.G., Wang, N., Mebane, C.A., 2007. An evaluation of freshwater mussel toxicity data in the derivation of water quality guidance and standards for copper. Environ. Toxicol. Chem. 26, 2066–2074.

Markl, J., 2013. Evolution of molluscan hemocyanin structures. Biochim. Biophys. Acta 1834, 1840–1853.

Mason, A.Z., Jenkins, K.D., 1995. Metal detoxification in aquatic organism. In: Tessier, A., Turner, D. (Eds.), Metal Speciation and Bioavailability in Aquatic Systems. J. Wiley & Sons, Chichester, UK, pp. 479–608.

Ng, T.Y.-T., Wang, W.-X., 2005. Dynamics of metal subcellular distribution and its relationship with metal uptake in marine mussels. Environ. Toxicol. Chem. 24, 2365–2372.

Nishikawa, T., Lee, I.S.M., Shiraishi, N., Ishikawa, T., Ohta, Y., Nishikimi, M., 1997. Identification of S100b protein as copper-binding protein and its suppression of copper-induced cell damage. J. Biol. Chem. 272, 23037–23041.

Ohkawa, H., Ohishi, N., Yagi, K., 1979. Assay for lipid peroxides in animal tissues by thiobarbituric acid reaction. Anal. Biochem. 95, 351–358.

Pan, K., Wang, .W..-X., 2009. Biodynamics to explain the difference of copper body concentrations in five marine bivalve species. Environ. Sci. Technol. 43, 2137–2143.

Pan, K., Wang, .W..-X., 2012. Reconstructing the biokinetic processes of oysters to counteract the metal challenges: physiological acclimation. Environ. Sci. Technol. 46, 10765–10771.

Peric, L., Perusco, V.S., Nerlovic, V., 2020. Differential response of biomarkers in the native European flat oyster *Ostrea edulis* and the non-indigenous Pacific oyster *Crassostra gigas* co-exposed to cadmium and copper. J. Exp. Mar. Biol. Ecol. 523, 151271.

Rainbow, P.S., 2002. Trace metal concentrations in aquatic invertebrates: why and so what? Environ. Pollut. 120, 497–507.

Rainbow, P.S., 2007. Trace metal bioaccumulation: models, metabolic availability and toxicity. Environ. Int. 33, 576–582.

Rainbow, P.S., Luoma, S.N., 2011a. Metal toxicity, uptake and bioaccumulation in aquatic invertebrates – Modelling zinc in crustaceans. Aquat. Toxicol. 105, 455–465.

Rainbow, P.S., Luoma, S.N., 2011b. Trace metals in aquatic invertebrates. In: Beyer, W. N., Meador, J.P. (Eds.), Environmental Contaminants in Biota: Interpreting Tissue Concentrations. Taylor and Francis Books, Boca Raton, FL, USA, pp. 231–252.

Rainbow, P.S., Smith, B.D., 2013. Accumulation and detoxification of copper and zinc by the decapod crustacean *Palaemonetes varians* from diets of field-contaminated polychaetes *Nereis diversicolor*. J. Exp. Mar. Biol. Ecol. 449, 312–320.

Regoli, F., Giuliani, M.E., 2014. Oxidative pathways of chemical toxicity and oxidative stress biomarkers in marine organisms. Mar. Environ. Res. 93, 106–117.

Rikans, L.E., Hornbrook, K.R., 1997. Lipid peroxidation, antioxidant protection and aging. Biochm. Biophys. Acta 1361, 116–127.

Roesijadi, G., 1980. Influence of copper on the clam *Protothaca staminea*: effects on gills and occurrence of copper-binding proteins. Biol. Bull. 158, 233–247.

Roesijadi, G., 1992. Metallothioneins in metal regulation and toxicity in aquatic animals. Aquat. Toxicol. 22, 81–114.

Tan, Q.-.G., Wang, .W..-X., 2012. Two-compartment toxicokinetic-toxicodynamic model to predict metal toxicity in *Daphnia magna*. Environ. Sci. Technol. 46, 9709–9715.

Tan, Q.-.G., Lu, S., Chen, R., Peng, J., 2019. Making acute tests more ecologically relevant: cadmium bioaccumulation and toxicity in an estuarine clam under various salinities modeled in a toxicokinetic-toxicodynamic framework. Environ. Sci. Technol. 53, 2873–2880.

Tipping, E., 1998. Humic ion-binding model VI: an improved description of the interactions of protons and metal ions with humic substances. Aquat. Geochem. 4, 3–48.

Van Straalen, N.M., Donker, M.H., Vijver, M.G., Van Gestel, C.A.M., 2005. Bioavailability of contaminants estimated from uptake rates into soil invertebrates. Environ. Pollut. 136, 409–417.

Veltman, K., Hendriks, A.J., Huijbregts, M.A.J., Wannaz, C., Jolliet, O., 2014. Toxicokinetic toxicodynamic modeling of Ag toxicity in freshwater organisms: whole-body sodium loss predicts acute mortality across aquatic species. Environ. Sci. Technol. 48, 14481–14489.

Vijayavel, K., Anbuselvam, C., Balasubramanian, M.P., 2007. Antioxidant effect of the marine algae *Chlorealla vulgaris* against naphthalene-induced oxidative stress in the albino rats. Mol. Cell. Biochem. 303, 39–44.

Vijver, M.G., van Gestel, C.A.M., Lanno, R.P., van Straalen, N.M., Peijnenburg, W.J.G.M., 2004. Internal metal sequestration and its ecotoxicological relevance: a review. Environ. Science. Technol. 38, 4705–4712.
Voets, J., Redeker, E.S., Blust, R., Bervoets, L., 2009. Differences in metal sequestration between zebra mussels from clean and polluted field locations. Aquat. Toxicol. 93, 53–60.
Wallace, W.G., Lee, B.G., Luoma, S.N., 2003. Subcellular compartmentalization of Cd and Zn in two bivalves. I. Significance of metal sensitive fractions (MSF) and biologically detoxified metal (BDM). Mar. Ecol. Prog. Ser. 249, 183–197.
Wang, W.-X., Rainbow, P.S., 2006. Subcellular partitioning and the prediction of cadmium toxicity to aquatic organisms. Environ. Chem. 3, 395–399.
Wang, M.J., Wang, W.X., 2008a. Cadmium toxicity in a marine diatom as predicted by the cellular metal sensitive fraction. Environ. Sci. Technol. 42, 940–946.
Wang, M.J., Wang, .W..-X., 2008b. Temperature-dependent sensitivity of a marine diatom to cadmium stress explained by subcellular distribution and thiol synthesis. Environ. Sci. Technol. 42, 8603–8608.
White, S.L., Rainbow, P.S., 1985. On the metabolic requirements for copper and zinc in molluscs and crustaceans. Mar. Environ. Res. 16, 215–229.